High-Frequency Broadband Rotor Noise

A. R. George* and Y. N. Kim†
Cornell University, Ithaca, N. Y.

A method has been developed to find the absolute spectral level of high frequency far field sound of a rotor in terms of random load fluctuations on the rotor blades. The analysis deals with frequencies where the radiated sound spectrum is smooth, i.e., above 300 to 400 Hz for a typical helicopter. This is in constrast to the low frequency regions where the spectrum is continuous but peaked near bladed passing harmonics. We first show that the smooth, broadband part of the spectrum corresponds to load fluctuations which are uncorrelated between blade passages. Then the spectral intensities from the individual blades are additive. A point load approximation with spanwise loading corrections is used and the blade loading spectrum is specifically derived for upwash fluctuations due to inflow turbulence. Analytic approximations are made to simplify the evaluation of certain integrals and series. The method is compared to the more general method of Homicz and George, where practical, and to published experimental data. The agreement between the two theories is excellent. The comparison to the experiments is good although it is not clear how to estimate the increase in intensity of atmospheric turbulence as it is distorted while being drawn into the rotor. The results indicate that atmospheric turbulence is perhaps the major contribution to broadband noise in hover. The approach is also applicable to other load fluctuation mechanisms.

I. Introduction

HELICOPTER rotors and fans generate complex acoustic signatures. A variety of mechanisms are responsible for the radiated sound and many of these mechanisms are only partly understood. In forward flight part of the radiated sound from a helicopter rotor is impulsive. This impulsive sound can be generated by blade vortex interactions, by high Mach number effects associated with high speed blade motion, and possibly by local unsteady transonic flows on advancing helicopter rotor blades. Another, more continuous, background sound is also generally present. It becomes the dominant sound in the absence of impulsive sound as, for example, in hovering helicopter flight.

The present work deals with this nonimpulsive component of rotor noise, which is often again divided into "discrete" or "rotational" noise and "broadband" noise. For example, consider the experimentally measured spectrum in Fig. 1.[1] If the spectrum of this sound is examined, it is seen to consist of a number of harmonically related finite width peaks at lower frequencies blending into a continuous spectrum at higher frequencies.

The sound radiated by a rotor at low to moderate subsonic speeds is essentially due to the moving and time varying pressure distributions on the blades. The first few blade passing harmonics in the sound spectrum can be attributed to steady azimuthally constant blade loads; this effect was originally explained by Gutin.[2] In order to explain the higher harmonics in the spectrum several authors have shown that time independent but azimuthally periodic loadings will generate a truly discrete or "line" acoustic spectrum.[3,4] They found that at high frequencies, the sound from even small amplitude high frequency loading harmonics can dominate that due to Gutin noise. However, this does not explain the origin of the high harmonic loadings necessary to produce the high frequency portions of experimental spectra nor the finite width of the low frequency spectral peaks and the transition to a smooth high frequency spectrum. In hover, nonuniform inflow due to recirculation, terrain, or fuselage effects can lead to periodic changes in loading on a rotating blade. However, the higher loading harmonics due to such nonuniformities decay rapidly. Measured helicopter spectra show the peak and valley shaped spectra up to several hundred Hertz, implying that the variations in loading exist over smaller time or distance scales than can be reasonably attributed to steady inflow variations. In addition, truly steady inflow variations would result in truly periodic loadings and, thus, true line spectra. By constrast, the experimental spectra show finite width peaks which become progressively broader at higher frequencies while they blend into each other at high enough frequencies. This indicates unsteady or random azimuthal loading variations. Thus, one concludes that the azimuthal loading fluctuations must be due to time varying phenomena.

II. High-Frequency Broadband Noise Mechanisms

A number of phenomena have been proposed which might contribute to such loading fluctuations. One significant source of loading fluctuations is the passage of the blades through turbulent velocity fluctuations in the rotor plane.[5] Under most daytime atmospheric conditions, the lower 1000 m of the atmosphere is turbulent due to the effects of at-

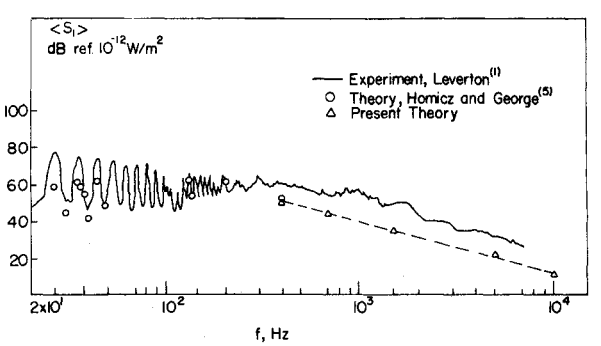

Fig. 1 Helicopter rotor noise spectrum measured by Leverton compared to theoretical calculations using undistorted turbulence estimates and Dryden spectrum. $\rho_o = 1.23$ kg/m^3, $\Omega = 4.3$ Hz, $C_o = 340$ m/sec, $(\overline{w^2})^{1/2} = 1$ m/sec, $r = 75.7$ m, $B = 2$, $M_o = 0.51$, $R_o = 6.4$ m, $M_c = 0.018$, $\Lambda = 0.57$ m, $c = 0.43$ m, $\phi = -11.5°$, $\mu = 6°$, $b = 8.5$ m.

Presented as Paper 76-561 at the Third AIAA Aero-Acoustics Conference, Palo Alto, Calif., July 20-23, 1976; submitted July 29, 1976; revision received Jan. 11, 1977.

Index category: Aircraft Noise, Aerodynamics (including Sonic Boom).

*Professor, School of Mechanical and Aerospace Engineering. Associate Fellow AIAA.

†Research Assistant, School of Mechanical and Aerospace Engineering. Student Member AIAA.

mospheric boundary-layer shear and bouyancy. A lifting rotor produces a mean downward velocity field which draws the atmospheric eddies through the rotor plane with a downward velocity V_c as sketched in Fig. 2. A typical root mean square value of turbulent velocity in the daytime atmosphere is of the order of 1.0 m/s. This velocity will then induce an angle-of-attack (or incidence) fluctuation of the order of 0.3° on a rotor blade traveling at 170 m/s. This magnitude of incidence fluctuation will induce load fluctuations on the order of one tenth of the steady blade loading. As atmospheric turbulence contains a spectrum of wavenumber components, the resulting loading spectrum affects the acoustic spectrum over the full range of frequencies, including both the low frequency peaks and the higher frequency continuous spectrum

The blades can also encounter turbulence due to the wakes of previous blades. The resultant increase of noise in this situation is well known.[6] However, most cases of interest involve a lifting rotor where wakes of previous blades will not significantly interact with following blades.

However, several other mechanisms exist for random loadings due to the flow around a single blade. If the blade boundary layers are largely laminar, certain tones are radiated which can be related to instability of the boundary layer or laminar wake.[7,8] However, this effect does not occur on most full scale rotors where the Reynolds number is greater than about 10^6 and the boundary layers are turbulent. However, as turbulence in a boundary layer passes near the trailing edge of the rotor, trailing-edge noise is generated.[9-12] Another possible related mechanism is the effect of the turbulence in the flow at a rotor tip where the tip vortex is initially forming. Lowson has reported some significant changes in radiated noise from a fan when the tip shape was changed slightly.[13]

III. Effects of Blade Rotation and Blade-to-Blade Correlation

Many of the possible mechanisms for sound generation have been investigated for the case of a single stationary airfoil in a moving stream.[14,15] However, in the case of rotating blades, the problem becomes more complicated. The fact that the blades are moving can be looked at in terms of Doppler shifts in frequency.[3] However, here we take the equivalent point of view that the variations of the pressure distribution associated with the presence or absence of the blade at various spatial locations become time variations as seen in observer coordinates. Thus, a range of frequencies are generated at blade passing harmonics $nB\Omega$ where n is the harmonic number, B the number of blades and Ω the shaft frequency.

A hovering or low forward speed rotor also modifies any ingested turbulence due to the distortion of fluid elements drawn into the rotor plane. This effect on turbulence structure has been experimentally studied by Hanson.[16] This effect can cause large changes in the properties of the turbulence. The calculation of these effects is difficult but experiments on the distortion of wind-tunnel turbulence in a contraction show large increases in turbulent energy in all three fluctuation velocity component directions.[17] (Note that the dimensionless intensity decreases due to the larger increase in mean velocity.) In Ref. 17, for example, the turbulent energies each increased by a factor of five in a 10:1 contraction.

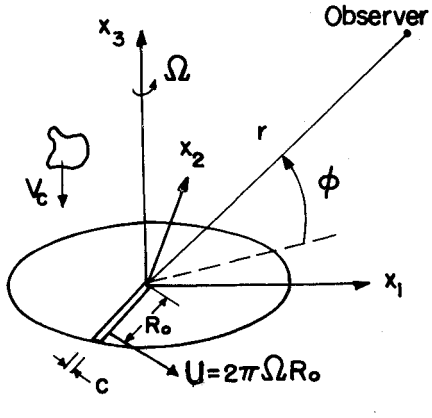

Fig. 2 Rotor geometry showing definitions of symbols and convection velocity of turbulent eddy.

Another rotor effect which does not occur for a stationary blade can be due to the correlation of loadings between blades. A sequence of blades passing through a given location will experience loading variations due to the passage of the turbulent eddies through the rotor plane. The blade loadings will vary rapidly or slowly depending on how small the eddies are. The blades can encounter parts of the same ingested turbulence eddies producing some correlation of the loadings between blades. For example, an atmospheric eddy of scale of 10 m will take the order of one second to be drawn through a typical hovering helicopter rotor with a convection velocity of 10 m/s. Thus, for two bladed rotor at 5.4 Hz, about twenty blade passages will encounter parts of the same eddy. This blade-to-blade correlation effect allows interference between waves generated by the various blades. The resulting amplitude modulation will then add sidebands to each blade passing harmonics. In particular, if the size of eddies becomes small, then they will generate high frequency blade loadings modulated to give wide sidebands around each blade passing harmonic.

IV. Previous Analysis

A unified analytical technique was presented for the prediction of acoustic radiation from aerodynamic rotors in Ref. 5. The model used there was that of an unducted axisymmetric rotor in hover, operating in some ambient turbulence pattern. The turbulence pattern was assumed given and frozen while it passed through the rotor face with a mean convection velocity V_c by virtue of rotor thrust. Initially, the blade was modelled as a point acoustic dipole at effective radius R_0. Later the analysis was corrected to include the effects of compressible unsteady aerodynamics and distributed loading on the blades. The analysis considered the effects of blade-to-blade correlation in a rigorous manner. Linearized small perturbation theory was used throughout.

Thus the previous analysis gave the far-field radiated spectrum for loading due to a turbulent upwash spectrum in the form

$$\langle S_l(f)\rangle \propto \int_{\xi_{MIN}}^{\infty} d\xi \Big[\sum_{n=n_1}^{n_2} \sum_{\ell=-\infty}^{\infty} G(\xi,n,\ell) J_{nB-\ell}^2\Big(\frac{f}{\Omega}\alpha\Big) \times J_\ell^2\Big(\frac{M_0}{M_c}\sqrt{\Big(\frac{V_c}{\Lambda\Omega}\Big)^2\xi^2-\Big(\frac{f}{\Omega}-nB\Big)^2}\Big)\Big] \quad (1)$$

where $\langle S_l(f)\rangle$, the acoustic spectrum, is expressed in the form of an integral over ξ, the turbulent velocity spectrum dimensionless wavenumber, and where the two series involving Bessel functions arise because of the resolution of the turbulence into polar coordinates and because of the Doppler shifts due to blade rotation. $G(\xi,n,\ell)$ includes the spectrum of the ingested turbulence and unsteady aerodynamic effect and the finite span effect of the blades. Λ is the turbulence integral scale, Ω is the shaft rotational frequency and B is the number of blades. M_o is the rotational Mach number of a blade at effective radius R_o as indicated in Fig. 2, M_c is the axial convection Mach number and $\alpha = M_o \cos\phi$ where ϕ is the observation angle measured from the rotor plane, V_c is the axial convection velocity of the turbulence.

The computations using Eq.(1) become prohibitively expensive for spectra past the range of about 500 to 1000 Hz for typical helicopter rotor parameters. This is because we need a

large range of load frequencies, Doppler shift terms, and azimuthal components terms due to the fact that the high frequency radiation is associated with the smaller turbulence eddies. This restriction also made it difficult to investigate the relative significance of other possible high frequency noise mechanisms.

V. Formulation

In the present work, we have developed a simpler method of calculation for the smooth high frequency part of the spectrum which takes advantage of the high frequency characteristics of the load fluctuations. The present analysis is specifically carried out for the important case of atmospheric turbulence induced loadings but can be modified to deal with other loading models.

We now show that the smooth part of the spectrum is primarily generated by loadings which are uncorrelated from blade to blade, allowing a direct summation of the intensities from the blades.

If we consider the interval of time Δt for equally spaced blades to pass a fixed point on the rotor plane, we find

$$\Delta t = \frac{2\pi R_o/B}{2\pi\Omega R_o} = \frac{1}{B\Omega}$$

On the other hand, the time scale for eddies to be convected past a given point in the rotor plane is:

$$T_\xi = \frac{\lambda_\xi}{V_c}$$

where λ_ξ is the eddy wavelength given by $2\pi\Lambda/\xi$. ξ is the turbulent wave number. Thus the ratio of blade passage time to convection time is given by

$$\frac{\Delta t}{T_\xi} = \frac{1}{2\pi}\frac{\xi V_c}{B\Lambda\Omega} \tag{2}$$

In our previous work we were able to show from detailed consideration of Eq.(1) that the frequency f_o beyond which the spectrum becomes smooth is given by[5]

$$f_o \simeq \frac{B\Omega(1+M_o/M_c)}{2(1-M_o\cos\phi)} \tag{3}$$

where ϕ is the observation angle measured from the rotor plane. We also were able to show that the values of ξ which make significant contributions to the spectrum at frequency f are

$$\frac{(f/\Omega)(1-M_o\cos\phi)}{(V_c/\Lambda\Omega)(1+M_o/M_c)} < \xi < \frac{(f/\Omega)(1+M_o\cos\phi)}{V_c/\Lambda\Omega}$$

Combining, we obtain the lower limit for ξ which makes significant contributions for $f > f_0$ as

$$\xi_{f_o} > B\Lambda\Omega/2V_c \tag{4}$$

Similarly, for $f >> f_0$ we obtain

$$\xi_f \gg B\Lambda\Omega/2V_c$$

Using this result, we find that $\Delta t/T_\xi >> 1$ when $f >> f_o$.

This result implies that the small turbulence eddies which generate the sound with $f > f_o$ completely pass through the rotor plane before the next blade arrives. Thus we can assume no blade-to-blade correlation. Similarly, if we consider other forms of broadband loading such as boundary-layer-trailing-edge interactions, etc., we see that if the blades are independent of other blades' wakes there is no reason to expect any correlation between loadings on separate blades. As a result, the radiation from separate blades will be uncorrelated.

Thus for broadband loadings we are able simply to add the uncorrelated sound power spectral densities of the radiation field from the B blades. The radiated spectral density of a single blade, considered as a rotating point load, can be expressed as shown by Ffowcs Williams and Hawkings[18] as

$$\langle S(x,f)\rangle = \frac{f^2}{4\rho c_o^3 r^2}\sum_{n=-\infty}^{\infty} D_r(f-n\Omega)J_n^2\left(\frac{f\alpha}{\Omega}\right) \tag{5}$$

where D_r is the power spectral density of the force fluctuation in the ϕ direction, f is frequency in Hz, $\alpha = M_o\cos\phi$, c_o is the sound speed, ρ is the density of acoustic medium and r is the distance between the observer and the rotor. Since the radiated pressure from a fluctuating force is proportional to $\partial/\partial t$ (force), which for a single frequency component is just 2πif (force), we see that the intensity spectrum contains the factor f^2. However, any given component of a load spectrum radiates over a range of Doppler shifted frequencies. Conversely, the acoustic spectrum at f involves load fluctuations at frequencies shifted from f by a range of harmonics $n\Omega$. The amplitudes of the Doppler shifted contributions are seen to be proportional to $J_n^2[f\alpha/\Omega]$ which is plotted below a sketch of $D_r(f-n\Omega)$ in Fig. 3. The value of $J_n^2[f\alpha/\Omega]$ becomes small for $n \gtrsim [f\alpha/\Omega]$. Thus the primary Doppler effects are shifts $\Delta f = n\Omega$ of less than approximately αf or using that $\alpha = M_o\cos\phi$ we obtain that the frequency shifts satisfy $\Delta f/f \lesssim M_o\cos\phi$ as would be expected from simple Doppler shift ideas.

Referring again to Fig. 3, we see that the spectrum of f is only affected by D_r over a range of frequencies of width $2fM_o\cos\phi$ around f. For $\phi \to 90°$, the on axis case, the radiation at f is only affected by the load spectrum at f as in the case of a stationary airfoil. However, for $M_o\cos\phi$ of order 0.5, as is typical for a helicopter, a large part of the load spectrum contributes to radiation.

The point load approximation made here is only exactly applicable in the limit of acoustic wavelength large compared to chord and rotor span. The spanwise loading distribution due to turbulent inflow is correlated over distance of the order of the inverse wave number of the particular incident turbulence component being considered and this effect is easily accounted for by assuming random phase between radiated sound from uncorrelated parts of the span.[5] The spanwise loading effect of other mechanisms can be treated similarly if their correlation lengths can be estimated.

Chordwise loading and noncompactness effects are quite important at high frequencies. Both the airfoil unsteady aerodynamic response and the acoustic radiations directivity are affected as has been discussed in Ref. 5 and more recently by Kaji[19] and Amiet.[15] In the present work we take advantage of the fact that the directivity of the radiation from rotating blades is largely averaged out for a fixed observer location. Thus, although the directivity of the radiation from a fixed airfoil changes from a dipole type $\sin^2\theta$ distribution to an edge type $\sin^2\theta/2$ distribution, the overall effect on rotor radiation can still be reasonably approximated by dipole directivity, for angle which are not too close to the rotor plane. For these angles, a rotor-angle-averaged correction can be used in future applications.

VI. Blade Loading due to Turbulence

We next find the lift loading on a blade moving relative to a fluid containing a homogeneous randomly varying upwash field w. We define coordinates fixed with respect to the fluid as x' and coordinates fixed with respect to the airfoil as x. We then write the four-dimensional Fourier representation of the turbulence upwash with respect to the fluid as

$$w(x',t) = \int \mathrm{d}^3v \int \mathrm{d}f\, F_w(v,f)e^{i2\pi v\cdot x'}e^{i2\pi ft}$$

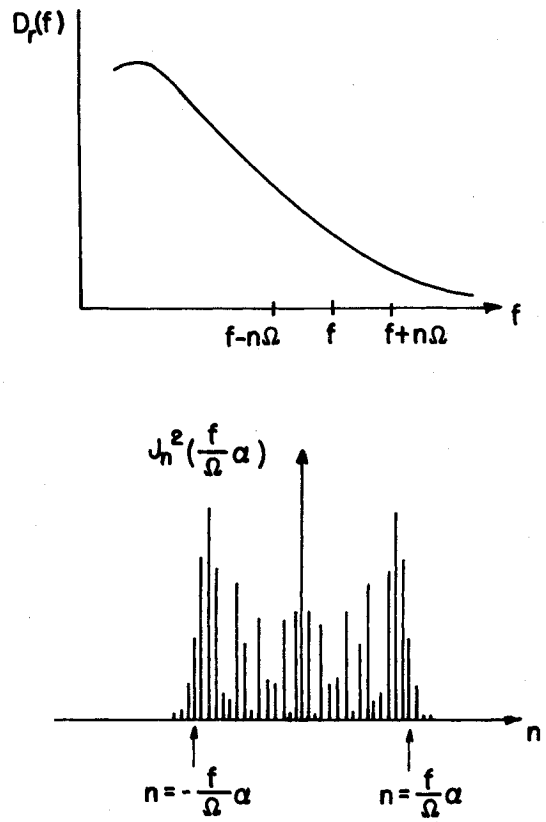

Fig. 3 Sketch of load spectrum and Doppler shift amplitude factors.

where f is the frequency and ν is the wave number vector of the turbulent fluctuations. Now if the blade moves with velocity Q with respect to the fluid where $Q=(U,O,-V_c)$, we have $x'=x-Qt$. Also we make Taylor's hypothesis that the turbulent upwash field is frozen, i.e., it does not vary during the time of a blade passage. In terms of the Fourier representation this is expressed as

$$F_w(\nu,f)=F_w(\nu)\delta(f)$$

Making these two substitutions we find the upwash expressed in blade fixed coordinates as

$$w(x,t)=\int d^3\nu\, F_w(\nu)e^{i2\pi(\nu\cdot x-\nu\cdot Qt)}$$

We now define the lift response function of the wing by

$$dl(\nu)=K(\nu_c,\nu_s)dw(\nu)$$

where ν_c and ν_s are wave number components in chordwise and spanwise directions, respectively. K is the aerodynamic lift response at a moving point of the rotor blade to a unit amplitude of turbulent upwash. Then we can express the lift on the blade as

$$l(t)=\int d^3\nu F_w(\nu)K(\nu_c,\nu_s)e^{-i2\pi\nu\cdot Qt}$$

This result can be applied to any isotropic or anisotropic $F_w(\nu)$ and for any Q. If we now assume $F_w(\nu)$ is isotropic, we can rotate our coordinates as shown in Fig. 4 so that the new x_1 axis is parallel to Q, and x_2 is along the span so that

$$l(t)=\int d^3\nu F_w(\nu)K(\nu_1,\nu_2)e^{i2\pi\nu_1 Qt}$$

where $Q=|Q|$.

In order to obtain the lift spectral density, we form the lift correlation

$$\overline{l(t)l^*(t+\tau)}=\int d^3\nu\int d^3\bar{\nu}\,\overline{F_w(\nu)F_w^*(\bar{\nu})}K(\nu_1,\nu_2)$$
$$\cdot K^*(\bar{\nu}_1,\bar{\nu}_2)e^{-i2\pi\nu_1 Qt}e^{+i2\pi\bar{\nu}_1 Q(t+\tau)}$$

where $\overline{\ }$ denotes an ensemble average. Taking its Fourier transform we can obtain the lift spectral density

$$\phi_{ll}(f)=\int\overline{l(t)l^*(t+\tau)}e^{-i2\pi f\tau}d\tau$$

Now for a statistically homogeneous field all Fourier components are uncorrelated unless their wave numbers are equal, thus we have

$$\overline{F_w(\nu)F_w^*(\bar{\nu})}=\phi_{ww}(\nu)\delta(\nu-\bar{\nu})$$

and the $\bar{\nu}$ integration gives

$$\phi_{ll}(f)=\int d^3\nu\int\phi_{ww}(\nu)\,|K(\nu_1,\nu_2)|^2e^{i2\pi(\nu_1Q-f)\tau}d\tau$$

But since

$$\int e^{i2\pi(\nu_1Q-f)\tau}d\tau=\delta(\nu_1Q-f)$$

we obtain

$$\phi_{ll}(f)=\frac{1}{Q}\int d\nu_2 d\nu_3\phi_{ww}\left(\frac{f}{Q},\nu_2,\nu_3\right)\left|k\left(\frac{f}{Q},\nu_2\right)\right|^2$$

Or in terms of a one-sided spectrum with $f\geq 0$

$$\phi_{ll_1}(f)=\frac{2}{Q}\int\int d\nu_2 d\nu_3\phi_{ww}\left(\frac{f}{Q},\nu_2,\nu_3\right)\left|K\left(\frac{f}{Q},\nu_2\right)\right|^2 \tag{6}$$

This result can be used with any K or ϕ_{ww}. In order to facilitate comparisons with Ref. 5, our present calculations use the same approximate K based on Osborne's asymptotic solution for the compressible extension of the two-dimensional Sears function.[20,5] It is given by

$$|K(\nu_1,\nu_2)|=\frac{1}{2}\rho Q\,bc\frac{2\pi}{(1-M_o^2)^{1/2}}$$
$$\cdot\frac{\left[J_o^2\left(\frac{M_o^2\pi c}{1-M_o^2}\nu_T\right)+J_1^2\left(\frac{M_o^2\pi c}{1-M_o^2}\nu_T\right)\right]^{1/2}}{\left[1+\frac{2\pi^2}{1-M_0^2}\nu_T\right]^{1/2}} \tag{7}$$

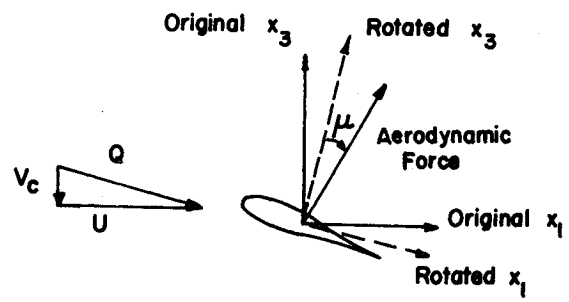

Fig. 4 Velocities relative to blade and original and rotated coordinates.

where $v_T = \sqrt{v_1^2 + v_2^2}$ and b is blade span and c is blade chord. J_o and J_1 are Bessel functions of order zero and one respectively.

The blade loading spectrum derived above is that for a fluctuating lift force which is actually oriented at a slight angle μ to the rotor axis, giving rise to small fluctuating torque components as well as the large thrust components. This angle is small for a helicopter rotor, typically 6°. Since the thrust is along the axis by definition, its contribution to the force in the direction of the observer is statistically stationary and is just given by $T\sin\phi$. On the other hand, the torque component in the observer direction is of order $T\tan\mu\cos\phi$ and varies in time due to blade rotation and thus is not statistically stationary. This complicates matters as Eq.(5) is strictly valid only for statistically stationary blade loading components. Since the angle μ is so small, the ratio of torque to thrust components $\tan\mu\cos\phi$ is not important in typical cases except near the rotor plane $\phi = 0$. Sample calculations using the method of Ref. 5 show spectrum changes of approximately one dB for ϕ as small as 27°, if the fluctuating torque components are included. Thus we have not included these effects in the present calculations and we use $D_r = \phi_{11}\sin^2\phi$.

The effect of spanwise correlation length on radiated intensity is accounted for by estimating the appropriate correlation lengths for atmospheric turbulence induced loads. For load fluctuations of frequency $f = v_1 Q$ the correlated length is order v_1^{-1}. Then if each patch of correlation length radiates independently, as previously discussed in Sec. IV, the radiated intensity correction can be approximated by $(1 + v_1 b)^{-1}$ (Ref. 5). Thus the final expression for radiated sound becomes in terms of one-sided power spectra

$$\langle S_1(x,f)\rangle = \frac{Bf^2}{4\rho c_o^3 r^2} \sum_{n=-\infty}^{n=+\infty} \frac{D_{r_1}(|f - n\Omega|) J_n^2\left(\frac{f}{\Omega}\alpha\right)}{(1 + bf/Q)} \tag{8}$$

where

$$D_{r_1}(f) = \frac{2\sin^2\phi}{Q} \cdot \int dv_2 dv_3 \phi_{ww}(f/Q, v_2, v_3) |K(f/Q, v_2)|^2 \tag{9}$$

In the present calculations, again in order to facilitate comparisons with Ref. 5, we will use the Dryden form of the spectrum

$$\phi_{ww}(v) = 64\pi^3 \overline{w}^2 \Lambda^5 \frac{v_1^2 + v_2^2}{(1 + 4\pi^2\Lambda^2 v^2)^3} \tag{10}$$

where $v^2 = v_1^2 + v_2^2 + v_3^2$, $\overline{w}^2$ is the mean square turbulence intensity, and Λ is the length scale in the corresponding correlation function:

$$R_{ww}(\epsilon_3) = \overline{w}^2 e^{(-|\epsilon_3|/\Lambda)}$$

In evaluating Eq. (9), the integration with respect to v_3 may be carried out analytically for the assumed form of ϕ_{ww} leaving the v_2 integration still to be carried out.

In principle one could now numerically evaluate the single integration and truncate the infinite sum remaining to obtain the radiated sound. In practice, since the integration must be done numerically, we are still faced with a formidable computation [although much less formidable than that of Eq.(1)]. In order to try to minimize the amount of computations, we looked at two further simplifications which are presented in Secs. VII and VIII.

VII. Evaluation of Series Expansion Method

Our first attempt at simplification was based upon expanding the loading component spectrum in a Taylor series which then enables us to analytically approximate the Bessel function sums. If we expand

$$D_r(f) = D_r(f_1) + D_r'(f_1)(f - f_1) + \frac{1}{2} D_r''(f_1)(f - f_1)^2 + \ldots$$

Substituting above expansion into Eq.(5) and using some Bessel function identities which we derived from some results of Watson,[21] we obtain[22]

$$\langle S(f_1)\rangle = \frac{f_1^2}{4\rho c_o^3 r^2}\left[\left\{D_r(f_1) + \frac{\alpha^2 f_1^2}{4} D_r''(f_1) + \frac{\alpha^4 f_1^4}{64} D_r^{(iv)}(f_1) + \frac{\alpha^6 f_1^6}{2304} D_r^{(vi)}(f_1) t \ldots\right\} + \left(\frac{\Omega}{\alpha f_1}\right)^2\left\{\frac{\alpha^4 f_1^4}{48} D_r^{(iv)}(f_1) + \frac{\alpha^6 f_1^6}{384} D_r^{(vi)}(f_1) + \ldots\right\} + \left(\frac{\Omega}{\alpha f_1}\right)^4\left\{\frac{\alpha^6 f_1^6}{1440} D_r^{(vi)}(f_1)\ldots\right\} + \ldots\right] \tag{11}$$

This result can be further manipulated and shown to be equivalent to the earlier results of Morfey and Tanna.[23]

In order to determine if this approach is useful in practical cases, we note that, except for near the axis ($\phi \simeq 90°$), for typical helicopters

$$\alpha = M_o \cos\phi \simeq 0.50, \quad \Omega \simeq 5\ Hz$$

and for broadband noise $f_1 \simeq 300$ Hz. Thus we see that for high frequencies we can neglect the $(\Omega/\alpha f_1)^2$ and higher order terms. We then are left with a series in α^2 with terms proportional to

$$f_1^s D_r^{(s)}(f_1)$$

If we consider the simplest case with a smooth high frequency behavior of D_r given by $D_r(f) = cf^{-m}$, we find that this series is only slowly converging for typical m's and $\alpha \simeq 0.5$ characteristic of helicopter rotors. For $\alpha \simeq 0.1$, which might correspond to a low speed fan or to near the axis of a helicopter, only one or two terms need be taken for the smooth spectrum case and it might be a useful approach. However, we must keep in mind that more typical load spectra due to trailing edge or tip loading fluctuations might not be as smooth and the series expansion would converge more slowly. Thus, we concluded that this approach is not very promising for general helicopter rotor applications.

VIII. Calculation Procedure

In order to numerically evaluate Eq.(8), we must be able to truncate the infinite sum with negligible error and numerically evaluate the v_2 integration for each term in the sum. Our second approach was to determine appropriated simplified methods and error estimates for these evaluations.

The basic idea of limiting the sum to a finite number of terms is due to the fact that $J_n(x)$ becomes small for $n >> |x|$. By comparing results with different n's we determined that the series could be truncated with less than one percent error if n ranged between

$$n_{\min}, n_{\max} = \mp 1.2 M_o |\cos\phi| f/\Omega$$

In the evaluation of the integral of the unsteady lift function and the upwash spectrum, the integration must be truncated at a finite wave number. For the case of interest the integral is of the form

$$\int_o^\infty dx \frac{(x^2+p^2)\{J_o(a[x^2+p^2]^{1/2})+J_1^2(a[x^2+p^2]^{1/2})\}}{\{1+2\pi^2 c(1-M_o^2)^{-1}(x^2+p^2)^{1/2}\}\{1+4\pi^2\Lambda^2(x^2+p^2)\}^{5/2}} \tag{12}$$

where

$$x=v_2,\ a=M_o^2\pi c/(1-M_o^2),\ p=(f-n\Omega)/Q$$

Our first estimates showed that although the integral decreased fairly rapidly for large x, in order to retain good accuracy the integral could not be truncated until a quite large value of x is reached. This large range of integration then required a large amount of computer time for evaluation of the integral. Thus we developed a method to evaluate the large x portion of the integral analytically using asymptotic representations of the factors in the integrand. Schematically, we write the integral as

$$\int_o^\infty g(x)dx \simeq \int_o^A g(x)dx + \int_A^\infty h(x)dx \tag{13}$$

where asymptotically, $g(x) \sim h(x)$ for $x \to \infty$. We found that for x large enough so that

$$a(x^2+p^2)^{1/2} > T \tag{14}$$

where T is a fixed number, that the Bessel functions become asymptotically

$$J_o^2(a[x^2+p^2]^{1/2})+J_1^2(a[x^2+p^2]^{1/2}) \sim \frac{2}{\pi a(x^2+p^2)^{1/2}}$$

and under the same condition

$$1+\frac{2\pi^2 c}{1-M_o^2}(x^2+p^2)^{1/2} \sim \frac{2\pi}{M_o^2}a(x^2+p^2)^{1/2}$$

and

$$1+4\pi^2\Lambda^2(x^2+p^2) \sim 4\pi^2\Lambda^2(x^2+p^2)$$

Using these approximations, the part of the integration from A to ∞ can be written as

$$\frac{1-M_o^2}{2^5\pi^9 c^2\Lambda^5 M_o^2}\int_A^\infty \frac{dx}{(x^2+p^2)^{5/2}} \tag{15}$$

This can be integrated analytically to obtain

$$\int_A^\infty \frac{dx}{(x^2+p^2)^{5/2}} = \frac{2}{3p^4} - \frac{A}{3p^2(A^2+p^2)^{3/2}} - \frac{2A}{3p^4(A^2+p^2)^{1/2}} \tag{16}$$

The number A is determined for all n from Eq.(14) as

$$A=\left[\left(\frac{T}{a}\right)^2 - P_{\min}\right]^{1/2} \tag{17}$$

where $P_{\min}=(f-n_{\max}\Omega)/Q$ was used to keep the estimate conservative. In our calculations we took $T=5$. For this value of T the errors involved in using the asymptotic form of the integrand were found to be less than one percent.

The integration

$$\int_o^A g(x)dx$$

was evaluated numerically using a variable interval size low order integration algorithm which was developed for badly behaved integrations by O'Hara and Smith.[24] The number of points were chosen in order to obtain accuracy of better than one percent.

It is clear from Eq.(17) that for higher frequencies A becomes smaller making computation easier, which is the opposite of the trend associated with computations based on Eq.(1). Thus, the present method is ideally suited to high frequency radiation calculations.

The Bessel functions were determined by a backward recurrence relation which obtains $J_{n-1}(x)$ from $J_n(x)$.[25]

IX. Calculations and Comparison with Experiments

At the present time there is no completely satisfactory experimental data known to the authors with which we can compare our theory. In addition to the need for accurate high resolution experimental spectra, simultaneous accurate measurements of the properties of the ingested atmospheric turbulence should be made. As no such data exist we compare the theory to two well-documented helicopter rotor measurements[1,26] and estimate the atmospheric turbulence properties from standard measurements.[27] The estimation of turbulence properties is quite straightforward except that it is not known how much the atmospheric turbulence is modified as it is distorted while being drawn into the rotor.

There are no arbitrary or empirical factors in our analysis and thus, our calculations predict absolute rather than relative levels. Figure 1 includes calculations made to compare the present high frequency method to the inverted rotor, tower experiments of Leverton. Leverton designed these tests to eliminate recirculation and the reingestion of the rotor wake by the rotor. In this case the atmospheric turbulence ingested by the rotor primarily originates between the ground level and the rotor height. As the integral scale Λ of atmospheric turbulence is proportional to distance from the ground, the turbulence ingested is quite inhomogeneous in this experiment. The rms turbulence intensity $(\overline{w^2})^{1/2}$ was estimated at 1 m/s and Λ at 0.57 m. The circles indicate calculations made using the method of Ref. 5, while the present method is indicated by triangles. The solid line indicates the variable bandwidth experimental data corrected to a 1.0 Hz bandwidth power spectral density using

$$\langle S_I(f)\rangle = SPL - 10\log_{10}\Delta f$$

where Δf is the experimental filter bandwidth.

The comparison shows excellent agreement with the method of Ref. 5 for the frequency of approximately 400 Hz, where both methods were applicable. The experiment and the computations show the same trend at high frequencies but the calculated absolute level is approximately 10 dB low. This could correspond to a change in turbulent rms velocity due to inflow distortion, or to our choice of turbulence model, as will be discussed below.

A comparison between theoretical calculations and the data of Johnson and Katz for a full scale helicopter are shown in Fig. 5. Again, the agreement between the earlier and the present theory is within 2 dB, where both methods can be applied. This difference is most likely due to the use of a rotationally averaged wave number approximation in the unsteady lift response function of Ref. 5. In the present case, where blade to blade correlations are zero, no such approximation was required. When the two theoretical methods were compared using the identical quasisteady aerodynamics, the agreement was within 0.3 dB.

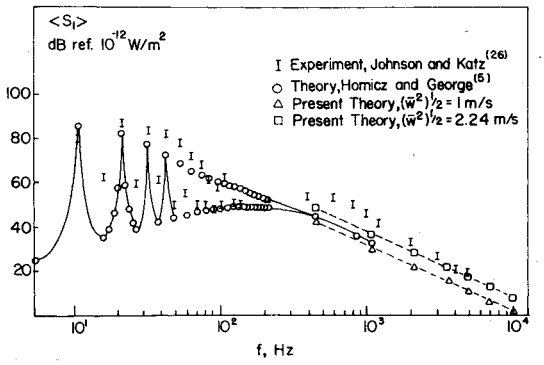

Fig. 5 Comparison of helicopter noise spectrum measurements of Johnson and Katz to theoretical calculations using Dryden spectrum with undistorted flow and assumed distorted inflow turbulent intensities. $\rho_o = 1.3$ **Kg/m**^{3}, $\Omega = 5.4$ **Hz**, $C_o = 330$ **m/sec**, $r = 66.75$ **m**, $B = 2$, $M_o = 0.55$, $R_o = 5.34$ **m**, $M_c = 0.027$, $\Lambda = 27.5$ **m**, $c = 0.53$ **m**, $\phi = -27°$, $\mu = 6°$, $b = 6.34$ **m**.

The atmospheric turbulence theory again shows the same trend with frequency as the experiment. The values of $(\overline{w^2})^{1/2}$ and Λ for the daytime atmosphere at the helicopter's altitude are estimated as one m/s and 27.5 m. These values do not take any distortion effects into account and the theoretical calculation are about 10 dB low.

Both theoretical calculations were made using the Dryden spectrum model of Eq.(10). This spectrum was originally used in Ref. 5, which was concerned with lower frequencies than the present analysis. The energy spectral density of the Dryden spectrum decays asymptotically for large v as v^{-2} while atmospheric turbulence characteristically decays as $v^{-5/3}$ in the inertial range. The use of the Karman spectrum model, which exhibits such a decay would probably be preferable. However, the effect of this turbulence spectrum on the radiated sound can be anticipated from the results presented in Ref. 28. Acoustic spectra were computed by the method of Ref. 5 and compared for turbulence spectra with v^{-2} and $v^{-1.02}$ asymptotic decays. Based on those results one would anticipate that the present calculations would be increased by about 3 dB at 1000 Hz and would decay slightly more slowly with frequency.

In order to show the possible effects of the distortion of the ingested turbulence, Fig. 5 also shows high frequency calculations for $(\overline{w^2})$ increased by a factor of five. This factor of five was not intended to be necessarily representative of this rotor, but was merely the value measured in the particular wind tunnel contraction experiments of Klein and Ramjee.[17] This factor increases the theoretical spectra by 7 dB, considerably improving the agreement with measurements. This calculation was carried out only to show the change of absolute level of acoustic spectrum due to an example of distorted turbulence. We need more complete information on the distortion of ingested turbulence including anisotropicity before being able to draw any definite conclusions.

In the present helicopter rotor applications, for frequencies near where the spectrum first becomes smooth, the computation time required per point using the method of Ref. 5 is of the order of thirty seconds CPU time on an IBM 370-168. For these frequencies this time can be decreased by a factor of one-half using the present method. Also, the earlier method requires an exponential increase in CPU time as the frequency is increased; at 1000 Hz the time required exceeds one minute. For higher frequencies the cost becomes prohibitive. The present method's computation time stays in the range between one to forty seconds for frequencies below 10,000 Hz.

X. Conclusions

A relatively simple method has been developed to calculate high frequency broadband rotor noise due to blade loading fluctuations. The present method modelled a rotor blade as an acoustic point dipole and included the effect of finite span. The correlation between blades was neglected based on the order of magnitudes of the physical effects. The method can be adapted to a range of statistically stationary load mechanisms but was specifically applied in this paper to atmospheric turbulence induced loadings. The method is much simpler than earlier methods where they both apply and has been economically applied to frequencies as high as 10,000 Hz for typical helicopter rotors. The good agreement with experiment supports the various approximations made and also supports the idea that atmospheric turbulence is perhaps the major cause of broadband noise in hover. Further theoretical investigation is needed on the change of inflow turbulence properties and on other blade load fluctuation mechanisms. Also further experimental work is needed on the effects of inflow on the turbulence ingested by low forward speed rotors and on inflow turbulence properties in general. Other fluctuating load mechanisms such as those in the rotor tip region also need further experimental investigation.

Acknowledgment

This research was sponsored by the U. S. Army Research Office DAHCO4-75-6-0120.

References

[1]Leverton, J. W., "The Noise Characteristics of a Large 'Clean' Rotor," *Journal of Sound and Vibration*, Vol. 27, 1973, pp. 357-376.

[2]Gutin, L., "On the Sound Field of a Rotating Propeller," NACA TM 1195, 1948.

[3]Lowson, M. V. and Ollerhead, J. B., "A Theoretical Study of Helicopter Noise," *Journal of Sound and Vibration*, Vol. 9, 1969, pp. 197-222.

[4]Wright, S. E., "Sound Radiation from a Lifting Rotor Generated by Asymmetric Disc Loading," *Journal of Sound and Vibration*, Vol. 9, 1969, pp. 223-240.

[5]Homicz, G. F. and George, A. R., "Broadband and Discrete Frequency Radiation from Subsonic Rotors," *Journal of Sound and Vibration*, Vol. 36, 1974, pp. 151-177.

[6]Scheiman, J., Hilton, A. and Shivers, J. P., "Acoustical Measurements of the Vortex Noise for a Rotating Blade Operating with and without its Shed Wake Blown Downstream," NASA TN D-6364, 1971.

[7]Fink, M. R., "Prediction of Airfoil Tone Frequencies," *Journal of Aircraft*, Vol. 12, Feb. 1975, pp. 118-120.

[8]Tam, C. K. W., "Discrete Tones of Isolated Airfoils," *Journal of the Acoustical Society of America*, Vol. 55, June 1974, pp. 1173-1177.

[9]Fink, M. R., "Experimental Evaluation of Trailing Edge and Incidence Fluctuation Noise Theories," *AIAA Journal*, Vol. 13, Nov. 1975, pp. 1472-1477.

[10]Hayden, R. E., "Noise from Interaction of Flow with Rigid Surfaces: A Review of Current Status of Prediction Techniques," NASA CR-2126, Oct. 1972.

[11]Ffowcs Williams, J. E. and Hall, L. H., "Aerodynamic Sound Generation by Turbulent Flow in the Vicinity of a Scattering Half Plane," *Journal of Fluid Mechanics*, Vol. 40, 1970, pp. 657-670.

[12]Chase, D. M., "Noise Radiated from an Edge in Turbulent Flow," *AIAA Journal*, Vol. 13, Aug. 1975, pp. 1041-1047.

[13]Lowson, M.V., Whatmore, A., and Whitfield, C.E., "Source Mechanisms for Rotor Noise Radiation," Loughborough University of Technology, Loughborough, England, Report TT7202, 1972.

[14]Sharland, J. J., "Sources of Noise in Axial Flow Fans," *Journal of Sound and Vibration*, Vol. I, March, 1964, pp. 302-322.

[15]Amiet, R. K., "Acoustic Radiation from an Airfoil in Turbulent Stream," *Journal of Sound and Vibration*, Vol. 41, 1975, pp. 407-420.

[16]Hanson, D. B., "Measurement of Static Inlet Turbulence," AIAA Paper 75-467, Hampton, Va., 1975.

[17]Klein, A. and Ramjee, V., "Effects of Contraction Geometry on Non-Isotropic Free-Stream Turbulence," *The Aeronautical Quarterly*, Vol. 24, Feb. 1973, pp. 34-38.

[18]Ffowcs Williams, J. E. and Hawkings, D. L., "Theory Relating to the Noise of Rotating Machinery," *Journal of Sound and Vibration*, Vol. 10, 1969, pp. 10-21.

[19]Kaji, S., "Noncompact Source Effect on the Prediction of Tone Noise from a Fan Rotor," *AIAA Progress in Astronautics and Aeronautics: Aeronautics: Fan Noise and Control; Duct Acoustics; Rotor Noise;* Editor: Ira R. Schwartz; Assistant Editors: Henry T. Nagamatsu and Warren C. Strahle, Vol. 44, MIT Press, Cambridge, Mass., 1976, pp. 55-81.

[20]Osborne, C., "Unsteady Thin Airfoil Theory for Subsonic Flow," *AIAA Journal*, Vol. 11, Feb. 1973, pp. 205-209.

[21]Watson, G. N., *A Treatise on the Theory of Bessel Functions*, Second Ed., Cambridge University Press, Cambridge, England, 1966, pp. 35-37.

[22]George, A. R. and Kim, Y. N., "High Frequency Broadband Rotor Noise," AIAA Paper 76-561, Palo Alto, Calif., 1976.

[23]Morfey, C. L. and Tanna, H. K., "Sound Radiation from a Point Force in Circular Motion," *Journal of Sound and Vibration*, Vol. 10, 1971, pp. 325-351.

[24]O'Hara, H. and Smith, F. J., "The Evaluation of Definite Integrals by Interval Subdivision," *Computer Journal*, Vol. 12, 1969, pp. 179-182.

[25]Luke, Y. L., "On Generating Bessel Functions by Use of the Backward Recurrence Formula," Aerospace Research Laboratories, Wright-Patternson Air Force Base, Ohio, Rept. 72-0030, Feb. 1972.

[26]Johnson, H. K. and Katz, W. M., "Investigation of the Vortex Noise Produced by a Helicopter Rotor," USAAMRDL, Technical Report 72-2, 1972.

[27]Lumley, J. L. and Panofsky, H. A., *The Structure of Atmospheric Turbulence*, Wiley, New York, 1964, pp. 135-137, 167-175.

[28]George, A. R., *et al.*, "Research on Helicopter-Rotor Noise," *Book of Proceedings*, Vol. I, Second Interagency Symposium on University Research in Transportation Noise, North California State University, Raleigh, June 5-7, 1974, pp. 328-345.